INSTITUTE OF PHYSICS PUBLISHING JOURNAL OF PHYSICS: CONDENSED MATTER

J. Phys.: Condens. Matter **13** (2001) 167–175 www.iop.org/Journals/cm PII: S0953-8984(01)15016-2

# Comparative study of hypersonic propagation in $YBa_2Cu_3O_{7-\delta}$ single crystals and thin films

**P Kuzel**[1], **C Dugautier and P Moch**

Laboratoire des Propriétés Mécaniques et Thermodynamiques des Matériaux, CNRS, Université Paris-Nord, Avenue J B Clément, 93430 Villetaneuse, France

Received 27 July 2000, in final form 9 October 2000

**Abstract**

Elastic properties of $YBa_2Cu_3O_{7-\delta}$ single crystals and thin epitaxial films were measured at room temperature by means of Brillouin scattering. The elastic stiffnesses, which reflect a pseudo-tetragonal symmetry of the elastic properties, were determined for both kinds of samples. For the single crystals, only small differences from the previously published data were found. For the thin films, a significant hardening of the shear stiffness $C_{55}$ (15%) was observed, in contrast with the softening usually obtained for many compounds.

## 1. Introduction

The high-frequency elastic properties of the high-temperature superconductor $YBa_2Cu_3O_{7-\delta}$ (YBCO) have been studied by means of ultrasonic techniques, neutron scattering measurements and, to a lesser extent, Brillouin light scattering spectroscopy. Most of the ultrasonic experiments were done on polycrystalline sintered ceramic bulk samples [1–5]: the reported data show a large dispersion of the observed stiffness constants which is probably related to differences in the preparation procedures which result e.g. in variations of the porosity of the samples. The elastic properties of YBCO single crystals were successfully measured using ultrasonic [6–8], neutron scattering [9] and Brillouin scattering experiments [10–13]; depending upon the particular study, distinct sets of stiffness constants were obtained, providing evidence of the elastic anisotropy of the structure. However, here again, the agreement between different experimental findings and their comparison with the estimates [14] is not completely satisfactory. Generally, a pseudo-tetragonal behaviour of the elastic properties is reported, but some papers conclude that there is a significant orthorhombic contribution [8, 13]. A non-negligible influence of the oxygen content on the elastic constants has been reported [15, 16]. Finally, some results on the elastic properties of YBCO thin films were obtained by means of ultrasonic techniques [17–19]. They only concern the relative changes of the surface acoustic wave velocities and attenuation near the superconducting phase transition. However, the elastic properties of YBCO thin films have not been completely determined so far.

[1] Present address: Institute of Physics, Academy of Sciences of the Czech Republic, Na Slovance 2, 182 21 Prague 8, Czech Republic.

0953-8984/01/010167+09$30.00  

The elastic properties are important characteristics of thin films: the amplitude of the elastic anisotropy is related to the quality of the epitaxial growth; quantitative comparison between the bulk and thin-film results allows one to evaluate the stresses near the substrate–thin-film interface. The study of YBCO thin films is also of practical interest, since they are successfully used as buffer layers for the epitaxial growth of ferroelectric thin films [20].

We investigated the long-wavelength surface acoustic phonons by means of Brillouin scattering. The spectra generally consist of a Rayleigh pseudo-surface mode, a set of modes guided within the thin film and longitudinal resonance features; they are analysed in terms of displacement correlation functions calculated near the sample surface [21–26]. This analysis provides a set of effective elastic constants, which are compared to those obtained for bulk single crystals.

## 2. Description of the scattering by surface modes

As is well known, the light is scattered by two physically distinct processes: (i) surface ripple and (ii) bulk elasto-optic coupling.

(i) The scattered radiation arising from the ripple is related to the autocorrelation function $g_{33}$ of the displacement component normal to the surface (denoted as $u_3$):

$$g_{33} \equiv \langle u_3(z=0)u_3(z=0)\rangle = \frac{kT}{\hbar\omega}\,\mathrm{Im}\{G_{33}(Q_\parallel,\omega)\}$$

where $G_{33}$ is a component of the elastic susceptibility tensor [26]. This expression assumes that the contribution of the top surface (air–thin film) is the leading one compared to the contribution of the deeper interfaces of the layered structure studied. Due to the large optical absorption of YBCO, this assumption is well justified for our experiments.

(ii) The above-mentioned ripple process is usually dominant for opaque materials; however, in some cases the elasto-optic contribution can be non-negligible, as observed in our spectra described in the next section. The corresponding scattered field is related to the strain-induced electric polarization:

$$P_i = -\varepsilon_{ij}\varepsilon_{kl}\,p_{ijmn}u_{mn}E_l$$

where $p_{ijmn}$ is the (fourth-rank) photo-elastic tensor and $\varepsilon_{ij}$ is the (second-rank) dielectric tensor; $u_{mn} = \partial u_m/\partial x_n$ is a displacement gradient term (the strain in the sample). The scattered radiation is then essentially related to a linear combination of the correlation functions of the displacement derivatives $\langle u_{mn}(z)u_{kl}(z')\rangle$ integrated over the whole sample. The terms of this linear combination are weighted by the photo-elastic coefficients. Due to the large optical absorption of YBCO (penetration depth <50 nm) the integration can be limited to a very thin layer close to the surface. Consequently, for the purposes of a rough evaluation, the correlation functions can be approximated by their values at the surface. For most of the crystals the $p_{ij}$-coefficients (in Voigt notation) with $i \leqslant 3$, $j \leqslant 3$ are significantly larger than the others. A careful examination of the expression providing the elasto-optic scattered intensity then allows one to conclude that the leading term is proportional to

$$g_{11} \equiv \langle u_1(z=0)u_1(z=0)\rangle = \frac{kT}{\hbar\omega}\,\mathrm{Im}\{G_{11}(Q_\parallel,\omega)\}.$$

Let us emphasize that the above susceptibility $G_{11}$ is expressed in the sagittal system of axes (following figure 1): $\boldsymbol{Q}_\parallel$ is parallel to the $x$-axis. Thus, for any particular crystal orientation, $G_{11}$ depends on an appropriate combination of the leading $p_{ij}$-terms. The evaluation of $g_{11}$ can then provide a semi-quantitative estimate of the expected inelastically scattered intensity.

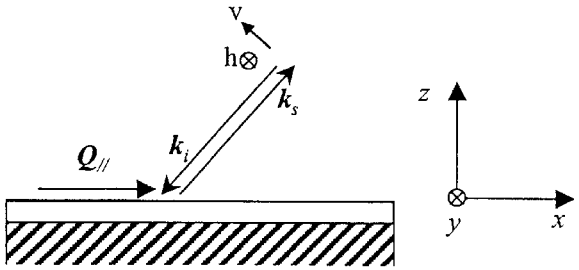


**Figure 1.** A schematic diagram of the scattering geometry.

In the following discussion we use the above approximations and we attempt to interpret the measured spectra using the elastic susceptibilities $G_{11}$ and $G_{33}$.

Let us briefly describe the spectral features related to the modes propagating along the $\boldsymbol{a}$-axis in orthorhombic crystals. One expects to observe:

(i) A Rayleigh surface mode (RSM) [27]. Both $g_{11}$ and $g_{33}$ contribute to the scattered intensity; the velocity of the RSM depends on the shear stiffness $C_{55}$ and, to a lesser extent, on $C_{11}$, $C_{13}$ and $C_{33}$.

(ii) A longitudinal surface resonance (called the high-frequency pseudo-surface mode: HFPSM) [28] related to the contribution of $g_{11}$. Its velocity depends mainly on $C_{11}$; the shape of this spectral feature also depends on $C_{13}$ and, to a lesser extent, on $C_{33}$. The dependence on $C_{55}$ is practically negligible.

(iii) Several guided modes (which only exist in layered structures) [27] corresponding to the poles of $g_{33}$. Their number, their velocities and their spectral intensities depend on the same elastic constants as the RSM mode ($C_{11}$, $C_{13}$, $C_{33}$ and $C_{55}$) and on the geometrical parameters (layer thickness); in usual experimental conditions they are much more sensitive to the thickness than the RSM mode.

For a more general propagation direction in the ($\boldsymbol{a}$, $\boldsymbol{b}$) plane the above-mentioned modes show an in-plane anisotropy. Assuming an approximately tetragonal structure, this anisotropy is characterized by the value of $C_{12} + 2C_{66}$. If the orthorhombicity is explicitly taken into account, the differences between the constants $C_{11}$ and $C_{22}$, $C_{13}$ and $C_{23}$, $C_{55}$ and $C_{44}$ produce additional contributions to the anisotropy.

## 3. Experimental results and discussion

The Brillouin spectra were obtained using a 2 × 3-pass tandem Fabry–Pérot interferometer; backscattering geometry with an excitation wavelength of 514.5 nm was used. All of the spectra were obtained with the v/v combination of polarizations of the incident/scattered light (see figure 1). In the v/h arrangement no Brillouin signal was observed.

### *3.1. Single crystals*

The ($1 \times 1 \times 0.1$ mm$^3$) single crystal studied was cut with the crystallographic $\boldsymbol{c}$-axis normal to the illuminated face ($\boldsymbol{c} \parallel \boldsymbol{z}$; see figure 1). The angle of incidence was varied from 30° to 65° and the direction of the wave vector $\boldsymbol{Q}_{\parallel}$ of the phonons was also scanned within the ($\boldsymbol{a}$, $\boldsymbol{b}$) plane. An example of a spectrum is given in figure 2. Two Brillouin lines were observed that were related to the RSM at low frequency and to the HFPSM [10, 28] at higher frequency. We

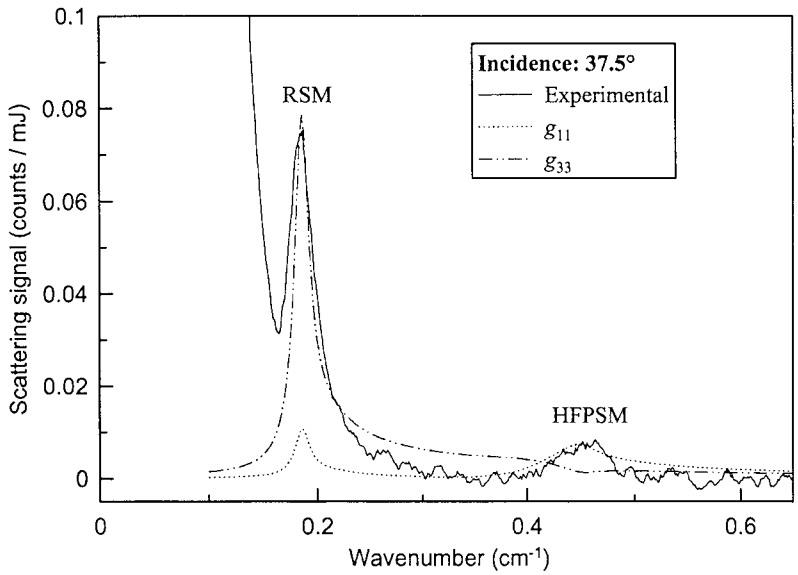


**Figure 2.** An example of a spectrum for the bulk YBCO single crystal; $g_{11}$ and $g_{33}$ are theoretical autocorrelation functions obtained using the elastic constants given in the text.

verified experimentally that the conventional bulk modes are not observed: this is in agreement with the statement that the elasto-optic scattering arises only from the proximity to the surface.

In principle, the whole set of measurements, fitted with the help of $g_{11}$ and $g_{33}$, depend on the whole set of non-vanishing elastic constants. However, not all of the constants can be unambiguously determined. First, we found that, within the experimental error, the crystal is practically tetragonal (i.e. $C_{11} \approx C_{22}$, $C_{13} \approx C_{23}$, $C_{44} \approx C_{55}$). The most precise evaluations are for

(i) $C_{11}$ which is closely related to the longitudinal resonance associated with a maximum of $g_{11}$ and
(ii) $C_{55}$ which mainly governs the position of the Rayleigh surface wave and provides a prominent maximum of $g_{33}$.

We found $C_{11} = 210 \pm 10$ GPa and $C_{55} = 38 \pm 2$ GPa, in relatively good agreement with the previously published values determined by Baumgart *et al*, also deduced from Brillouin spectra [10] ($C_{11} = 211$ GPa and $C_{55} = 35$ GPa). Our value of $C_{55}$ is slightly higher than that in [7]: we observed experimentally a larger value of the Rayleigh wave velocity ($v_R = 2370$ m s$^{-1}$ to be compared to 2270 m s$^{-1}$). The values of $C_{33}$ and $C_{13}$ cannot be precisely derived from our data: the contributions of $C_{33}$ and $C_{13}$ to the correlation functions can compensate each other to some extent. If we take 160 GPa for $C_{33}$, as proposed in [10], we obtain a rough evaluation of $C_{13} \approx 80$ GPa in reasonable agreement with neutron scattering results (100 GPa, derived in [9]). Notice that a very different value of $C_{33}$ (61 GPa) was proposed in [7]: this value does not allow a satisfactory fit of our spectra and therefore we did not retain it. In contrast with those of $C_{13}$ and $C_{33}$, the evaluation of $C_{55}$ is rather accurate: no reasonable variation of the other elastic constants can induce a shift of $C_{55}$ larger than 2 GPa. $C_{12}$ and $C_{66}$ cannot be obtained independently from our experiments: one has access only to $C_{12} + 2C_{66}$. We find $C_{12} + 2C_{66} = 250 \pm 10$ GPa which provides a value of the in-plane anisotropy ($C_{11} - C_{12} - 2C_{66}$) of about $-40$ GPa. This is in excellent agreement with [6] provided that

the value of $C_{11}$ (not measured in [6]) is taken equal to 210 GPa: it would then follow from the experimental results reported in [6] that $C_{66} = 102$ GPa, $C_{12} = 46$ GPa. Finally, let us mention that disagreements persist between our values and some published results [8, 13] which indicate a strong orthorhombic anisotropy.

### *3.2. Thin films*

We used a 540 nm YBCO epitaxial layer prepared by laser ablation on a MgO(001) single-crystal substrate. We measured its thickness using a scanning electron microscope with precision of about 30 nm. The YBCO layer consists of highly oriented crystallites with their $c$-axis normal to the film ($c$-domains) and with a high in-plane texture showing a fourfold symmetry. The sample does not contain any $a$-domains as verified by an x-ray diffraction study. The Brillouin scattering experiments were performed for various angles of incidence as well as for various in-plane orientations of the sample. The spectra obtained are rather rich (see figure 3): one observes a low-frequency surface mode, a series of Sezawa guided modes at intermediate frequencies and, finally, a complicated feature, which cannot be accounted for by the ripple contribution, near the expected longitudinal resonance frequency. Figure 4 shows the measured propagation velocities of the observed modes as functions of $Q_\parallel$ (which is scanned through the variation of the angle of incidence). The fits of the experimental data are also shown: they represent the positions of the maxima of $g_{11}$ and $g_{33}$. These fits allowed us to determine the values of four elastic constants for the YBCO thin film studied ($C_{55}$, $C_{11}$, $C_{33}$ and $C_{13}$). In figure 4 we also show the values of some important characteristic velocities: $v_T$(MgO) represents the upper threshold of the velocities of the guided modes in the YBCO film; $v_T$(YBCO) is the calculated velocity of the bulk transverse mode related to $C_{55}$: it determines the low-velocity threshold of the guided modes. Finally, $v_L$(YBCO) is the calculated velocity of the bulk longitudinal mode related to $C_{11}$: it roughly provides the

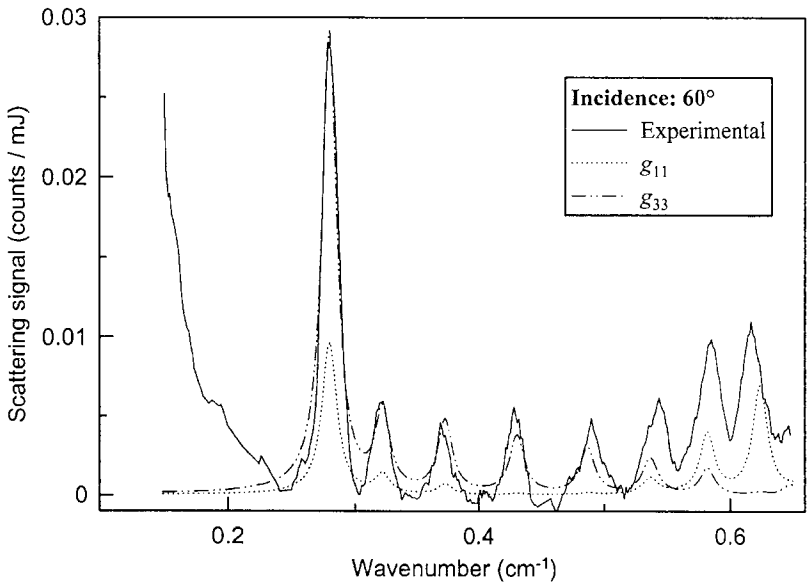


**Figure 3.** An example of a spectrum for the thin-film YBCO/MgO structure; $g_{11}$ and $g_{33}$ are theoretical autocorrelation functions obtained using the elastic constants given in the text.

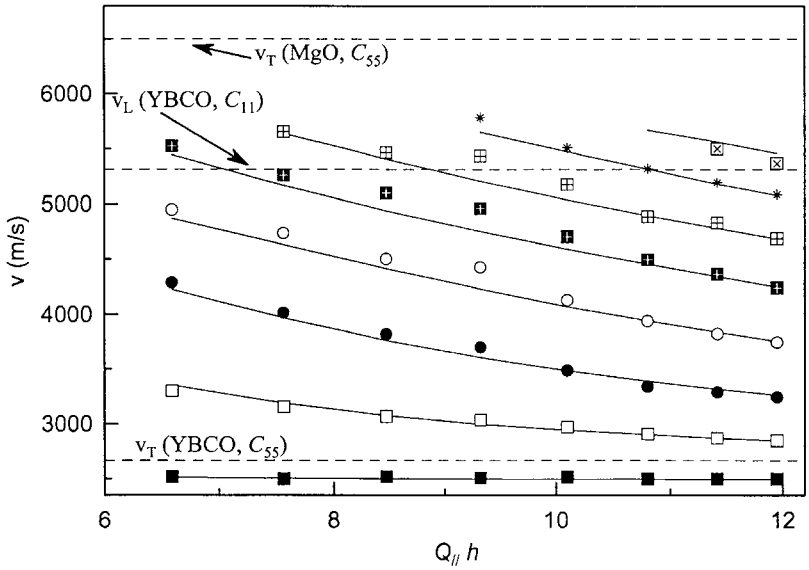


**Figure 4.** Propagation velocities of the modes observed in the YBCO/MgO structure (YBCO thickness: $h = 540$ nm) as a function of $Q_{\parallel}h$; $\boldsymbol{Q}_{\parallel}$ is parallel to the crystallographic $a$-axis. Points: measured values; full lines: positions of the maxima of the $g_{11}$- and $g_{33}$-functions; dashed lines: threshold velocities of the guided modes.

position of the longitudinal resonance. The velocities relative to YBCO were calculated using the values of the elastic constants obtained for the thin film studied.

Figure 5 shows the in-plane anisotropy of the observed modes obtained for an angle of incidence equal to 50°. The theoretical fits are also shown for comparison. Notice that not only the frequencies but also the scattered intensities depend on the orientation, as theoretically expected. The dotted curves of the theoretical fits correspond to orientations for which the appropriate maxima of the correlation functions are very small or vanish. Consequently, the scattered intensity is expected to be very small there. The agreement between the theory and the experiment is good: it validates the tetragonal approximation for the elastic properties of the YBCO thin film. The fit provides a value of 260 GPa for $C_{12} + 2C_{66}$, which is close to that obtained for the bulk sample.

Finally, we have noticed that the quality of the Brillouin spectra depends strongly on the preparation procedure and on the choice of substrate. Thus, when we proceeded to a Brillouin study of two YBCO epitaxial films (280 nm and 500 nm) grown by laser ablation on $SrTiO_3$:Nb substrates, we did not meet with success: the spectra obtained showed a signal-to-noise ratio six times lower than that for the above-described spectra of a YBCO/MgO sample. On the other hand, we obtained good quality Brillouin spectra with a two-layer $PbTiO_3$/YBCO/$SrTiO_3$:Nb structure. Their analysis, which gives access to the elastic properties of the $PbTiO_3$ films, will be published elsewhere. Here we only mention that the analysis cannot be performed in the absence of quantitative data on the YBCO sublayers; we found that the elastic constants derived from the present study of YBCO/MgO samples can be successfully used to determine the elastic properties of the $PbTiO_3$ films studied, thus allowing for a satisfactory interpretation of the spectra of these bilayered structures.

The elastic constants obtained for the thin film as well as for the bulk sample are summarized in table 1. When we compare our results for the bulk single crystal to the previously

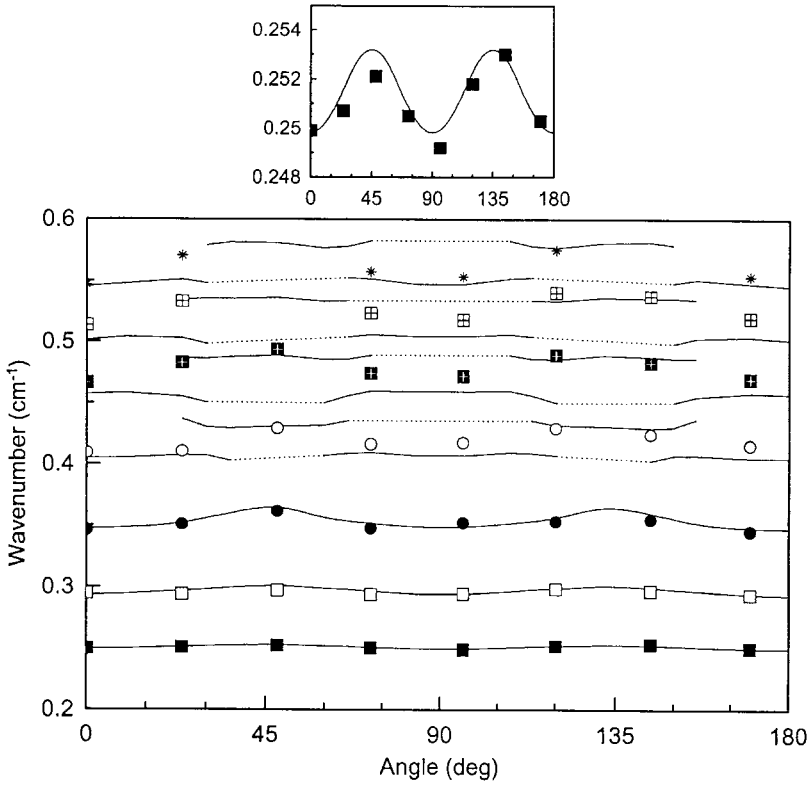


**Figure 5.** In-plane anisotropy of the modes observed in the YBCO/MgO structure. Incidence angle: 50°. Full lines: simulations with $g_{11}$- and $g_{33}$-functions. Dotted lines: regions where the scattered intensity of a particular mode vanishes. Inset: the Rayleigh surface mode on an enlarged scale.

**Table 1.** Room temperature elastic constants of the YBCO thin film and of the bulk single crystal deduced from the present Brillouin study.

| Elastic constant | Single crystal (GPa) | Thin film (GPa) |
|---|---|---|
| $C_{11} = C_{22}$ | 210 | 200 |
| $C_{33}$ | 160* | 160* |
| $C_{13} = C_{23}$ | 80 | 80 |
| $C_{55} = C_{44}$ | 38.5 | 44.5 |
| $C_{12} + 2C_{66}$ | 250 | 260 |

* Values taken from [10].

published ones, we conclude that our measurements validate the published values and choices for $C_{11}$, $C_{33}$, $C_{12}$ and $C_{66}$ [10, 17], indicating to elastic properties in agreement with a tetragonal symmetry. The comparison of the results obtained for the bulk sample and for the thin film indicates small differences in $C_{11}$ and $C_{12} + 2C_{66}$, which are, however, mainly related to the experimental uncertainties.

On the other hand, the thin film exhibits a significant hardening of $C_{55}$ (15%) with respect to the bulk sample. This behaviour is mainly deduced from the increase of the RSM velocity. The effect is clearly larger than the experimental errors; note that the velocity of the slow

transverse wave determined from the bulk sample data ($v_T$(bulk) $= 2460$ m s$^{-1}$) is even smaller than the RSM velocity measured in the thin film ($v_R$(thin) $= 2500$ m s$^{-1}$).

One finds in the literature a number of examples, e.g. metallic layers and multi-layers, where shear strains play an important role in the elastic properties of thin-film structures [29–32, 24]. The changes of effective elastic constants are mostly related to the breakdown of the elastic properties in interfacial layers or in grain boundaries. This generally results in a softening of the shear elastic constants with respect to those of the bulk; this softening usually becomes stronger when the layer thickness decreases. However, a slight hardening of the shear elastic constants has been observed for some thin films (e.g. in the case of nickel or permalloy; see [24]), but a satisfactory interpretation is still lacking. The hardening of $C_{55}$ found for YBCO thin layers then appears to be rather surprising but is not exceptional. It does not seem to be directly related to significant strains near the substrate–film interface. Although the YBCO/MgO lattice mismatch is as high as 8%, the value of the thin-film YBCO lattice parameter $c$ does not differ from the bulk value by more than 1% as verified by means of x-ray experiments. Moreover, the presence of an eventual interfacial layer between MgO and YBCO would not significantly influence the velocity of RSM, since the penetration depth of this mode is significantly smaller than the layer thickness: the RSM amplitude thus practically vanishes near the thin-film/substrate interface. From the study of polycrystalline bulk samples it has been shown that the effective elastic constants strongly depend upon the porosity [5, 33]: assuming that the thin films studied show a non-negligible porosity, one would expect a softening of the shear elastic constant in contrast to our results. Finally, a significant hardening of the shear modulus when the oxygen concentration increases has been observed in YBCO [15, 16]; we had no facilities to directly evaluate $\delta$ but, from indirect evidence related to other experimental studies performed on samples produced under the same conditions, it is clear that the difference in $\delta$ cannot be large enough to account for the measured hardening in our thin film. To conclude, the interpretation of this effect remains an open problem.

## Acknowledgments

The authors thank A Grishin, M G Karkut and J-P Chaminade for providing the YBCO thin films and single-crystal samples.

## References

[1] Ewert S, Guo S, Lemmens P, Stellmach F, Wynants J, Arlt G, Bonnenberg D, Kliem H, Comberg A and Passing H 1987 *Solid State Commun.* **64** 1153
[2] Bishop D J, Ramirez A P, Gammel P L, Batlogg B, Rietman E A, Cava R J and Millis A J 1987 *Phys. Rev.* B **36** 2408
[3] Lang M, Lechner T, Riegel S, Steglich F, Weber G, Kim T J, Lüthi B, Wolf B, Rietschel H and Wilhelm M 1988 *Z. Phys.* B **69** 459
[4] Bhattacharya S, Higgins M J, Johnston D C, Jacobson A J, Stokes J P, Goshorn D P and Lewandowski J T 1988 *Phys. Rev. Lett.* **60** 1181
[5] Ledbetter H M, Austin M W, Kim S A and Lei M 1987 *J. Mater. Res.* **2** 786
[6] Saint-Paul M and Henry J Y 1989 *Solid State Commun.* **72** 685
[7] Kim T J, Kowalewski J, Assmus W and Grill W 1990 *Z. Phys.* B **78** 207
[8] Lei M, Sarrao J L, Visscher W M, Bell T M, Thompson J D and Migliori A 1993 *Phys. Rev.* B **47** 6154
[9] Reichardt W, Pintschovius L, Hennion B and Collin F 1988 *Supercond. Sci. Technol.* **1** 173
[10] Baumgart P, Blumenröder S, Erle A, Hillebrands B, Güntherodt G and Schmidt H 1989 *Solid State Commun.* **69** 1135
[11] Aleksandrov V V, Velichkina T S, Voronkova V I, Diakonov A M, Syrnikov P P, Yakovlev I A and Yanovskii V K 1989 *Phys. Lett.* A **142** 307

[12] Aleksandrov V V, Velichkina T S, Voronkova V I, Yakovlev I A and Yanovskii V K 1990 *Solid State Commun.* **73** 559
[13] Zouboulis E, Kumar S, Welp U, Chen C H, Chan S K, Grimsditch M, Downey J and McNeil L 1992 *Physica* C **190** 329
[14] Ledbetter H and Lei M 1990 *J. Mater. Res.* **5** 241
[15] Lemmens P, Honnekes C, Brakmann M, Ewert S, Cornberg A and Passing H 1989 *Physica* C **162** 452
[16] Lin S, Lei M and Ledbetter H 1993 *Mater. Lett.* **16** 165
[17] Saint-Paul M, Pourtier F, Pannetier B, Villegier J C and Nava R 1991 *Physica* C **183** 257
[18] Lee S-G, Chi C-C, Koren G and Gupta A 1991 *Phys. Rev.* B **43** 5459
[19] Stenger M, Baumhoff S, Prieur J-Y, Joffrin J and Contour J-P 1998 *Eur. Phys. J.* B **2** 177
[20] Karkut M G, Le Marrec F, Maréchal C, Steinseth R K, El Marssi M, Farhi R, Dellis J L and Portemer F 1999 *Ferroelectrics* **226** 261
[21] Loudon R 1978 *Phys. Rev. Lett.* **40** 581
[22] Loudon R 1978 *J. Phys. C: Solid State Phys.* **11** 403
[23] Djemia P, Roussigné Y, Dugautier C, Ganot F and Moch P 2000 to be published
[24] Djemia P 1998 *PhD Thesis* Université Paris-Nord
[25] Velasco V R and Garcia-Moliner F 1980 *J. Phys. C: Solid State Phys.* **13** 2237
[26] Velasco V R and Garcia-Moliner F 1980 *Solid State Commun.* **33** 1
[27] Farnell G W 1970 Properties of elastic surface waves *Physical Acoustics* vol 6, ed W P Mason and R N Thurston (New York: Academic) p 109
[28] Camley R E and Nizzoli F 1985 *J. Phys. C: Solid State Phys.* **18** 4795
[29] Carlotti G, Fioretto D, Giovannini L, Socino G, Pelosin V and Rodmacq B 1992 *Solid State Commun.* **81** 487
[30] Carlotti G, Fioretto D, Giovannini L, Socino G, Rodmacq B and Pelosin V 1991 *Ultrasonics Symp. Proc.* vol 2, pp 1079–82
[31] Carlotti G, Montone A, Petrillo C and Antisari M V 1991 *J. Phys.: Condens. Matter* **5** 4611
[32] Subramanian S, Sooryakumar R, Prinz G A, Jonker B T and Idzerda Y U 1994 *Phys. Rev.* B **49** 17 319
[33] Ledbetter H, Lei M, Hermann A and Sheng Z 1994 *Physica* C **225** 397